

## SIMULATION OF VARIOUS FRACTURE MODELS BY VARYING GEOMETRICAL PARAMETERS USING TAGUCHI'S DOE

## SIMULACIJA RAZNIH MODELA LOMA VARIRANJEM GEOMETRIJSKIH PARAMETARA PRIMENOM TAGUČI PRISTUPA PROJEKTOVANJA EKSPERIMENATA

Originalni naučni rad / Original scientific paper  
UDK /UDC:

Rad primljen / Paper received: 9.02.2022

Adresa autora / Author's address:

<sup>1)</sup> Department of Mechanical Engineering, GM Institute of Technology, Davangere, Karnataka, India

<sup>2)</sup> Department of Mechanical Engineering, Jain Institute of Technology, Davangere, Karnataka, India

\*email: [saleemsabdoddamani@gmail.com](mailto:saleemsabdoddamani@gmail.com)

<sup>3)</sup> Department of Mechanical Engineering, SJM Institute of Technology, Chitradurga, Karnataka, India

<sup>4)</sup> Department of Mechanical Engineering, University BDT College of Engineering, Davangere, Karnataka, India

### Keywords

- fracture toughness
- $a/W$  ratio
- Taguchi's method
- CT specimens

### Abstract

*In the current fracture study, the notable Irwin's work utilizes the Westergaard theory and indicates that, for elastic materials, the displacement and stress in the vicinity of the crack tip is related to strain energy release rate and represented by a constant  $K$ . The main aim of the research work is to find the stresses and displacements near the crack-tip using a finite element simulation tool ANSYS®. In this work, models used for simulations are single edge notch specimen, central crack, compact tension specimens with geometric parameters  $a/W = 0.40, 0.45, \text{ and } 0.50$ , and thickness of specimen is considered to be 7, 10, and 12 mm. For the said parameters, Taguchi's design of experiments (DOE) has been carried out. Von-Mises stress is lowest for  $a/W = 0.40$  for almost all specimens except compact tension specimen. For the compact tension specimen, the von-Mises stress remains constant for  $a/W = 0.45$  to  $0.50$ . Hence, it will be the designers' flexibility to select any value of  $a/W$  ratio between 0.45 to 0.50.*

### INTRODUCTION

Failure investigation is the way toward gathering and evaluating the available data to decide the reason for the failure, regularly with the objective of deciding restorative activities or responsibility. It is a significant control in numerous parts of assembling industry, for example, the electronic hardware business, where it is an imperative instrument utilized in the advancement of new product and also the upgrading of existing ones. The failure study process depends on gathering failed components for resulting assessment of the reason or reasons for failure utilizing a wide range of strategies, particularly microscopy and spectroscopy. Non-destructive testing (NDT) strategies are significant on the grounds that the failed items are unaffected by examination, so assessment in some cases begins utilizing these techniques.

### Ključne reči

- žilavost loma
- odnos  $a/W$
- Taguchi metoda
- CT epruvete

### Izvod

*U istraživanju loma, razmatranjem radova Irvina, primećuje se teorija Vestergarda, gde se govori da kod elastičnog materijala, pomeranja i naponi u okolini vrha prsline zavise od brzine oslobađanja energije deformacija što je predstavljeno konstantom  $K$ . Cilj istraživanja je određivanje napona i pomeranja u okolini vrha prsline primenom alata ANSYS® za simulacije na bazi metode konačnih elemenata. U radu su korišćeni modeli za simulaciju tipa epruvete sa ivičnim zarezom, centralnom prslinom, kompaktne epruvete za zatezanje sa parametrima  $a/W = 0,40, 0,45$  i  $0,50$ , a debljine epruvete se uzima da je 7, 10 i 12 mm. Sa ovim parametrima primenjena je Taguchi metoda projektovanja eksperimenata (DOE). Najmanji fon-Mizes napon se dobija za  $a/W = 0,40$  za skoro sve epruvete osim za kompaktnu epruvetu za zatezanje. Kod kompaktne epruvete za zatezanje, fon-Mizes napon ostaje konstantan za  $a/W = 0,45$  do  $0,50$ . Zato projektant ima slobodu u izboru vrednosti odnosa  $a/W$  između 0,45 do 0,50.*

Like FEM, the method for area discretization of CS-FEM is as yet dependent on elements, however, the shape of elements could be increasingly adaptable when the extreme distorted concave, tile or polygonal element can be utilized. Right now, standard bilinear quadrilateral elements, otherwise called the Q4 elements for FEM, would be received for developing of foundation mesh. Here we will present the shape work assessment and assembly of stiffness matrix for CS-FEM.

An element is a numerical connection that characterizes how the degrees of freedom of a node identify with the next. These elements can be line, area, or solid. It additionally relates how the deflections make stresses.

Mohammed et al. /1/ have worked on fracture properties, like fracture toughness and nominal strength of glass fibre reinforced epoxy laminate and are very important especially

when using cohesive zone model. Various finite element methods (FEM) were used by many researchers to analyse the fracture related problems such as edge-based smoothed finite element (ES-FEM) /2/ using the specially adopted five node crack tip element, s-version FEM (s-FEM) which is a fully automatic fatigue crack growth simulation system /3/, cell-based smoothed finite element (CS-FEM) /4/ uses the virtual crack closure integral technique (VCCT) for evaluating stress intensity factors and crack propagation modelling and an embedded finite element method (E-FEM) has been utilized to simulate /5/ the two-dimensional fracture processes.

Sham Prasad et al. /6/ listed different methods to analyse the fracture energy and its suitability in solving the intralaminar fracture toughness of polymer matrix composites.

Noury /7/ uses finite element method to characterize the cracked bridge roller bearing. A two-dimensional cracked roller with edge-cracked disk is modelled and is subjected to radial compressive load and has been analysed to compare the obtained results and the data presented in literature. Razavi /8/ has worked on fatigue crack initiation/growth in the S690 steel alloy using single edge notch tension (SENT) specimens both experimentally and numerically.

Many methods have been developed to test the fracture toughness of the material such as: compact tension (CT), single edge notch bend (SENB), indentation techniques, circumferential notched tensile (CNT) specimens etc. These testing methods were used /9/ to determine the fracture toughness of the aluminium-graphite composite material. From the comparison it is found that all the methods agree with each other. Seitzl et al. /10/ have used finite element software to determine the stress intensity factor and the stress near the crack tip by wedge splitting test (WST) specimen, by applying several boundary conditions.

Doddamani et al. /11/ use ANSYS tool to simulate the fracture toughness for a metal matrix composite. Analysis results have been compared with the experimental results. Fracture toughness by using finite element method was done by various authors. Different authors /12-16/ studied different methods of finite element techniques to determine the mechanical/fracture behaviour of materials such as impact specimen /12/, SEB specimen /13/, tensile test specimen /14/. Zhou /15/ worked on 3D FEM simulations of silicon particle reinforced aluminium (SiCp/Al). Similar other finite element methods were utilized to analyse the crack-tip plastic zone /16/, to evaluate the fracture toughness /17-19/.

American society for testing and materials (ASTM) prescribed many standard specimens to test the fracture toughness. Among them CT, SENB specimens were widely used by many authors. As per ASTM standards /20-21/, the prescribed crack length to width ( $a/W$ ) ratio is 0.4 to 0.55, where 'a' is crack length in mm; 'W' is specimen width in mm. This range of the  $a/W$  ratio ensures the linear elastic loading and plain strain conditions.

From the above literature survey, we found very few researchers have worked on fracture analysis. The main objective of this work is to find displacement and stresses at the crack tip using von-Mises criterion in a finite element tool /22/. ANSYS® software has been utilized to estimate

the same using many models such as single edge notch, centre crack, compact tension specimens /23-31/ for the geometric parameter crack length to width ratio i.e.  $a/W = 0.40, 0.45, \text{ and } 0.50$ , and specimen thickness 7, 10, and 12 mm. An attempt has been made to validate the results of the FE analysis with the statistical ones using the Taguchi's analysis. The obtained stress at the crack tip is compared with the theoretically available crack-tip plastic zone shapes estimated from the elastic solutions and the Von Mises yield criterion for plain stress or plain strain condition.

## MODEL GENERATION

PLANE82 (shown in Fig. 1a) is a higher order variant of the four node 2-D element (PLANE42). It gives increasingly exact outcomes to mixed (quadrilateral-triangular) automatic meshes and can tolerate irregular shapes without as much loss of accuracy. The 8-noded element has perfect displacement shapes and is appropriate to model curved boundaries.

To encourage displaying of two correspondent confronts, a little opening of the crack should be made. A prescribed geometry of the opening is demonstrated in Fig. 1b.

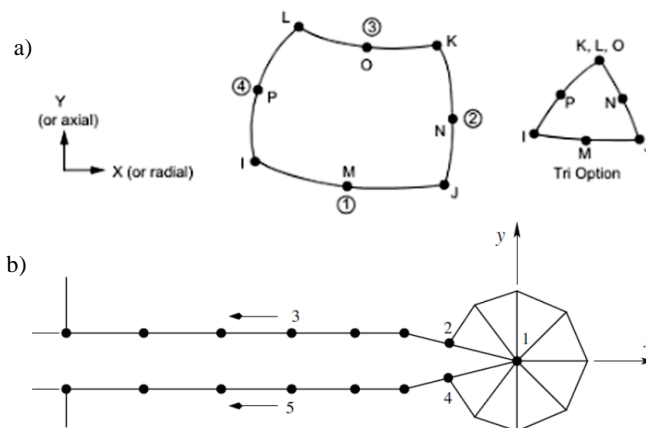


Figure 1. a) PLANE82 geometry; b) nodes around the crack tip /11/.

The 8-node elements are characterised by 8 nodes having 2 DOF at every node: interpretations in the nodal  $x$  and  $y$  directions. The component might be utilised as a plane component or as an axis-symmetric component.

Table 1. Taguchi's design of experiments L9 orthogonal array.

Case	Spec.	$a/W$ ratio	Thickness (mm)	Load at failure (kN)
1	SENT	0.40	7	2.58
2	SENT	0.45	10	2.39
3	SENT	0.50	12	2.17
4	CC	0.40	10	3.45
5	CC	0.45	12	3.33
6	CC	0.50	7	3.12
7	CT	0.40	12	4.49
8	CT	0.45	7	4.21
9	CT	0.50	10	3.38

The component has stress stiffening, large deflection, plasticity, creep, swelling, and extensive strain abilities. Different printout alternatives are additionally accessible. SOLID185 is a higher order version of the four node, 3D element (PLANE182). Using the KCALC command, stress

intensity factor in the region of crack may be calculated using linear elastic fracture mechanics analysis. This analysis utilizes a fit of the nodal displacement at the crack tip.

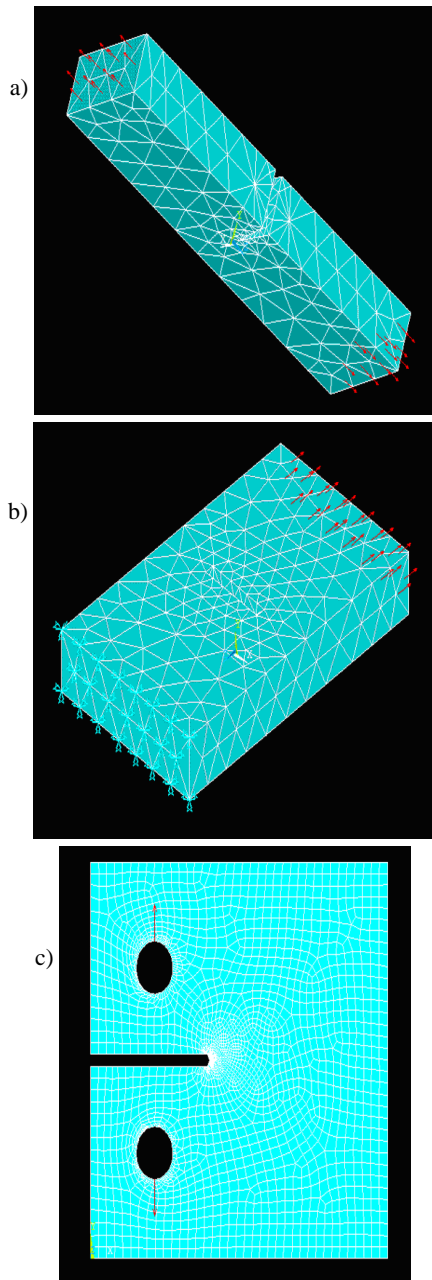


Figure 2. Finite element models of different specimens: a) SEN tension specimen; b) centre crack specimen; c) CT specimen.

The geometric model is created in ANSYS® for the Taguchi's design of experiments. The finite element models are built using Solid185 elements, as shown in Fig. 2. Key-points and area are created with concentrated keypoint at the crack tip. The model is meshed, with symmetric boundary conditions and the loads are applied before solving the problem. The finite element model is built using Solid185 elements, crack tip and nodes around the crack tip for the specimens shown in Fig. 2. Table 1 lists the L9 orthogonal array of the Taguchi's design of experiments also the load at failure.

## RESULTS AND DISCUSSIONS

Using finite element (FE) simulation, the displacement and von-Mises stresses are determined and noted for the SENT, CC, and CT specimens. Results of the simulation are given in Table 2.

Table 2. Input parameters for Taguchi's analysis.

Case	Spec.	$a/W$	Thickness (mm)	von-Mises stress (MPa)	max. displacement (mm)
1	SENT	0.40	7	243	0.0154
2	SENT	0.45	10	266	0.0196
3	SENT	0.50	12	248	0.0183
4	CC	0.40	10	271	0.0200
5	CC	0.45	12	301	0.0222
6	CC	0.50	7	299	0.0201
7	CT	0.40	12	247	0.0182
8	CT	0.45	7	279	0.0181
9	CT	0.50	10	268	0.0198

After analysing all the cases it is observed that the displacement and stress values are minimal for  $a/W = 0.4$ . Lesser  $a/W$  ratio indicates lesser crack length, due to which the specimen can withstand the higher loading conditions. Therefore, the lesser crack length will give the smaller displacement and stress values for the given load. For CC specimens, at higher  $a/W$  ratios, displacement follows the same trend as others, but only stress values are minimal. This is because plain strain condition exists in the range  $a/W = 0.45$  to  $0.50$ . At this range, specimen thickness exceeds the plane strain condition; hence stresses acting on the specimen will be lesser and almost follow a constant trend.

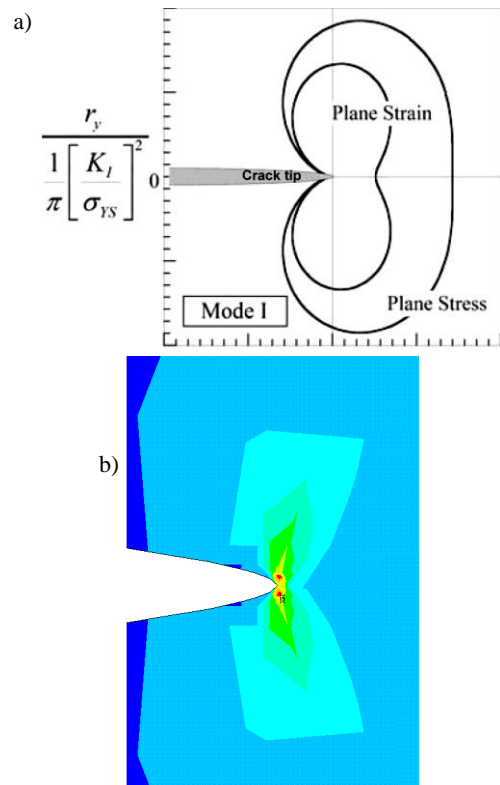


Figure 3. a) Theoretical shapes of mode I crack-tip plastic zone,  $r_p/2l$ ; b) stress around crack tip indicating plane strain fracture toughness.

The experimentally computed  $K_q$  is drawn with respect to different thickness for Al6061-9 % graphite composites. Figure 3b demonstrates the variation of  $K_q$  versus thickness for different Al6061-graphite composites. It is seen that the  $K_q$  reduces with increment in  $B/W$  proportions and is found to stay consistent for  $B/W \geq 0.4$ . This consistent estimation of  $K_q$  for  $B/W \geq 0.4$  prevails the plane strain fracture toughness ( $K_{Ic}$ ) of the composite.

The shape of the plastic zone and stress at the crack tip is expressed theoretically for mode I. This estimation is the result of elastic solutions and the von Mises yield criterion. From Fig. 3, it can be observed that there is a significant change in the shape for plane stress and plane strain conditions. The range of  $a/W$  ratio prescribed by ASTM fulfil the plane strain condition.

The shape of the plastic zone at the crack tip indicates plane stress and plane strain condition, as shown in Fig. 3a. From Fig. 3b it is clear that the shape of the von-Mises stresses is similar to that in Fig. 3a. Hence, the results obtained by FE simulation are in close relation with the theoretical approach. The analysis of fracture models is done successfully by using FE simulation software and it provides good correlation between FE results and the theoretical approach. Hence, the prescribed fracture models are used for analysis in FE simulation software. It is also recommended to use the simulation software for fracture toughness investigations which in turn reduces the cost and time.

#### TAGUCHI'S ANALYSIS

The displacement and von-Mises stress obtained from FE analysis are the input functions for Taguchi's analysis and ANOVA. Taguchi's analysis is carried out for the L9 orthogonal array and results are shown in Fig. 4.

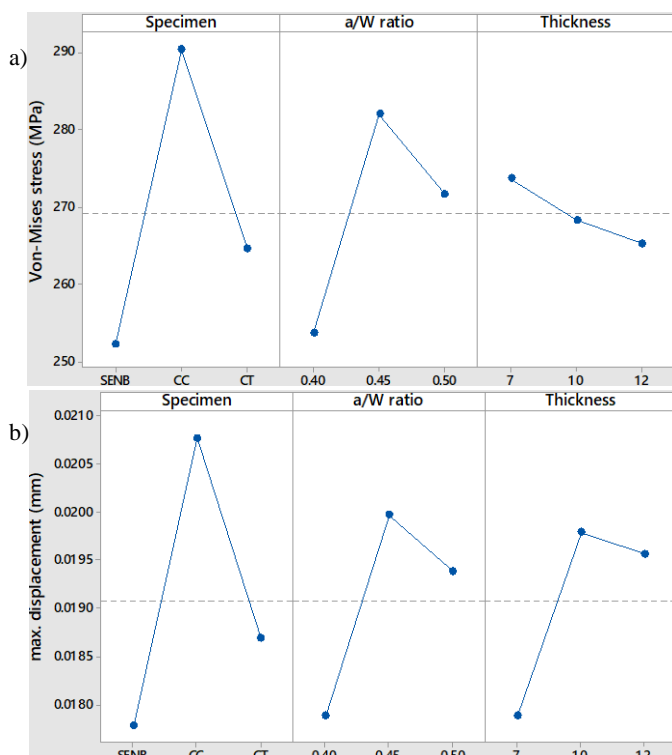


Figure 4. a) Main effects plot for von-Mises stress; b) main effects plot for maximal displacement.

Table 3 shows the ANOVA (analysis of variance) from which the percentage contribution of each parameter is analysed. From Table 3 (a and b) it is observed that the specimen used will impact more on the von-Mises stress and displacement. This is due to the influence of specimen geometry. Other than the  $a/W$  ratio, specimen thickness will have more influence. The error percentage is 0 to 1.2 %.

Table 3a. ANOVA for von-Mises stress.

Source	DF	Adj SS	F-value	P-value	% contribution
specimen	2	2254.89	51.77	0.019	62.0
$a/W$ ratio	2	1233.56	28.32	0.034	33.9
thickness	2	106.89	2.45	0.290	2.9
error	2	43.56	-	-	1.2
total	8	3638.89	-	-	100.0

Table 3b. ANOVA for max. displacement.

Source	DF	Adj SS	F-value	P-value	% contribution
specimen	2	0.000014	32.86	0.03	51.8
$a/W$ ratio	2	0.000007	16.34	0.058	25.9
thickness	2	0.000006	15.18	0.062	22.3
error	2	0	-	-	0.0
total	8	0.000027	-	-	100.0

Regression equations obtained from the analysis of von-Mises stress and displacement are given in Eq.(1) and Eq. (2), respectively,

$$\sigma_{\text{von}} = 204.3 + 180a/W - 1.68 \cdot \text{thickness} \quad (1)$$

$$\delta_{\text{max}} = 0.00882 + 0.0151a/W + 0.000359 \cdot \text{thickness} \quad (2)$$

The positive sign in Eqs. (1) and (2) indicates that the increment in the respective parameter increases the stress and thickness. However, increment in the  $a/W$  ratio increases the stress and displacement. The negative sign in Eq.(1) indicates the increment in specimen thickness reduces the stress. It is obvious that increases in thickness increases the area and thus stress reduces. The same has been shown in Fig 4a.

Comparison of experimental outcomes and the statistical results determined from the regression model is given in Table 4. It is observed that FE simulation and statistical results are in close agreement with each other with the error percentage 1 to 12 %. This gives the validation of FE simulation outcomes with the statistical outcomes.

Table 4. Comparison of FE simulation- with statistical results.

Case	von-Mises stress (MPa)			Max. displacement (mm)		
	FE simul.	Statist.	% error	FE simul.	Statistical	% error
1	243	265	8.1	0.0154	0.01737	11.1
2	266	269	0.9	0.0196	0.01921	2.1
3	248	274	9.5	0.0183	0.02068	11.5
4	271	260	4.2	0.0200	0.01845	7.7
5	301	265	11.9	0.0222	0.01992	10.3
6	299	283	5.5	0.0201	0.01888	6.1
7	247	256	3.6	0.0182	0.01917	5.0
8	279	274	2.0	0.0181	0.01813	0.1
9	268	278	3.4	0.0198	0.01996	1.0

#### CONCLUSIONS

Fracture analysis of single edge notch specimen, centre crack specimen, and compact tension specimen are successfully carried out using FE simulation. The von-Mises stress is lowest for  $a/W = 0.4$  for almost all of the specimens, hence, this can be generally selected and preferred as best

choice among others. For the centre crack specimen, the von-Mises stress remains constant for  $a/W = 0.45$  to  $0.50$ . Hence, it will be the designer flexibility to select any value of  $a/W$  ratio between  $0.45$  to  $0.50$ . It is also clear from the fracture models that at higher  $a/W$  ratio, the higher will be the stress and lower will be the toughness. From Taguchi's analysis it is identified that the specimen geometry impacts more on the induced stresses and displacement than the  $a/W$  ratio and specimen thickness.

## REFERENCES

- Mohammed, Y., Hassan, M.K., Abu El-Ainin H., Hashem, A.M. (2013), *Fracture properties of glass fiber composite laminates and size effect*, Sch. J Eng. Tech. 1(1): 13-26.
- Chen, L., Liu, G.R., Jiang, Y., et al. (2011), *A singular edge-based smoothed finite element method (ES-FEM) for crack analysis in anisotropic media*, Eng. Fract. Mech. 78(1): 85-109. doi: 10.1016/j.engfracmech.2010.09.018
- Kikuchi, M., Wada, Y., Shintaku, Y., et al. (2014), *Fatigue crack growth simulation in heterogeneous material using s-version FEM*, Int J Fatigue, 58: 47-55. doi: 10.1016/j.ijfatigue.2013.04.022
- Zeng, W., Liu, G.R., Jiang, C., et al. (2016), *An effective fracture analysis method based on the virtual crack closure-integral technique implemented in CS-FEM*, Appl. Math. Modell. 40(5-6): 3783-3800. doi: 10.1016/j.apm.2015.11.001
- Riccardi, F., Ejona, K., Richard, B. (2017), *A step-by-step global crack-tracking approach in E-FEM simulations of quasi-brittle materials*, Eng. Fract. Mech. 170: 44-58. doi: 10.1016/j.engfracmech.2016.11.032
- Sham Prasad, M.S., Venkatesha, C.S., Jayaraju, T. (2011), *Experimental methods of determining fracture toughness of fiber reinforced polymer composites under various loading conditions*, 10(13): 1263-1275. doi: 10.4236/jmmce.2011.1013099
- Noury, P., Eriksson, K. (2017), *Determination of stress intensity factors for cracked bridge roller bearings using finite element analyses*, Eng. Fract. Mech. 169: 67-73. doi: 10.1016/j.engfracmech.2016.10.018
- Razavi, N., Ayatollahi, M.R., Sommitsch, C., Moser, C. (2017), *Retardation of fatigue crack growth in high strength steel S690 using a modified stop-hole technique*, Eng. Fract. Mech. 169: 226-237. doi: 10.1016/j.engfracmech.2016.11.013
- Doddamani, S., Kaleemulla, M. (2019), *Comparisons of experimental fracture toughness testing methods of Al6061-graphite particulate composites*, J Fail. Anal. Preven. 19(3): 730-737. doi: 10.1007/s11668-019-00652-8
- Seitl, S., Veselý, V., Routil, L. (2011), *Two-parameter fracture mechanical analysis of a near-crack-tip stress fields in wedge splitting test specimens*, Comput. Struct. 89(21-22): 1852-1858. doi: 10.1016/j.compstruc.2011.05.020
- Doddamani, S., Kaleemulla, M. (2016), *Indentation fracture toughness of aluminum 6061-graphite composites*, Int. J Fract. Damage Mech. 1(1): 40-46.
- Chen, G., Huang, X. (2016), *Simulation of deformation and fracture characteristics of a 45 steel Taylor impact specimen*, Engng. Trans. 64(2): 225-240.
- Kawabata, T., Tagawa, T., Kayamori, Y., et al. (2017), *Plastic deformation behavior in SEB specimens with various crack length to width ratios*, Eng. Fract. Mech. 178: 301-317. doi: 10.1016/j.engfracmech.2017.03.029
- Chen, D.-C., Chang, D.-Y., Chen, F.-H., Kuo, T.-Y. (2018), *Application of ductile fracture criterion for tensile test of zirconium alloy 702*, Scientia Iranica B, 25(2): 824-829. doi: 10.24200/sci.2018.20174
- Zhou, F., Molinari, J.-F., Li, Y. (2004), *Three-dimensional numerical simulations of dynamic fracture in silicon carbide reinforced aluminum*, Eng. Fract. Mech. 71(9-10): 1357-1378. doi: 10.1016/S0013-7944(03)00168-1
- Sharanaprabhu, C.M., Kudari, S.K. (2010), *Analysis of crack-tip plastic zone in a Compact Tensile Shear (CTS) specimen*, Frat. ed Integ. Strut. 14: 27-35. doi: 10.3221/IGF-ESIS.14.03
- Guo, X., Chang, K., Chen, L.Q., Zhou, M. (2012), *Determination of fracture toughness of AZ31 Mg alloy using the cohesive finite element method*, Eng. Fract. Mech. 96: 401-415. doi: 10.1016/j.engfracmech.2012.08.014
- Mohammed, Y., Hassan, M.K., Hashem, A.M. (2012), *Finite element computational approach of fracture toughness in composite compact-tension specimen*, Int. J Mech. Mechatr. Eng. 12(4): 57-61.
- Vavrik, D., Jandajsek, I. (2014), *Experimental evaluation of contour J integral and energy dissipated in the fracture process zone*, Eng. Fract. Mech. 129: 14-25. doi: 10.1016/j.engfracmech.2014.04.002
- ASTM E 399-17, Standard Test Method for Linear-Elastic Plane-Strain Fracture Toughness  $K_{Ic}$  of Metallic Materials, ASTM International, 2017.
- Anderson, T.L., Fracture Mechanics - Fundamentals and Applications, 3<sup>rd</sup> Ed., Taylor & Francis Group, Boca Raton, 2013.
- Rajesh, A.M., Doddamani, S., Kaleemulla, M.K., Barath, K.N. (2020), *Dry sliding wear simulation of hybrid aluminum metal matrix composites*, Adv. Compos. Hybrid Mater. 3(1): 120-126. doi: 10.1007/s42114-020-00133-9
- Doddamani, S., Wang, C., Jinnah, M.S.M., Kowser, Md.A. (2021), *Fracture analysis of AA6061-graphite composite for the application of helicopter rotor blade*, Frattura ed Integrità Strutturale, 15(58): 191-201. doi: 10.3221/IGF-ESIS.58.14
- Begum, Y., Bharath, K.N., Doddamani, S., et al. (2020), *Optimization of process parameters of fracture toughness using simulation technique considering aluminum-graphite composites*, Trans. Indian Inst. Metals, 73(12): 3095-3103. doi: 10.1007/s12666-020-02113-5
- Guddhur, H., Naganna, C., Doddamani, S. (2021), *Taguchi's method of optimization of fracture toughness parameters of Al-SiCp composite using compact tension specimens*. An Int. J Optimiz. Control: Theories & Appl. (IJOCTA), 11(2): 152-157. doi: 10.11121/ijocta.01.2021.00990
- Doddamani, S., Kaleemulla, M. (2018), *Effect of graphite addition on the fracture and fatigue crack growth behaviour of Al6061-graphite*, Struct. Integ. Life, 18(3): 185-192.
- Doddamani, S., Kaleemulla, M. (2019), *Effect of aging on fracture toughness of Al6061-graphite particulate composites*, Mech. Adv. Compos. Struct. 6(2): 139-146. doi: 10.22075/mac.2019.16436.1177
- Doddamani, S., Kaleemulla, M. (2017), *Experimental investigation on fracture toughness of Al6061-graphite by using Circumferential Notched Tensile Specimens*, Frattura ed Integrità Strutturale, 11(39): 274-281. doi: 10.3221/IGF-ESIS.39.25
- Doddamani, S., Kaleemulla, M. (2019), *Effect of thickness on fracture toughness of Al6061-graphite*, J Solid Mech. 11(3): 635-643. doi: 10.22034/jsm.2019.666695
- Doddamani, S., Kiran, J.O., Kaleemulla, M., Bakkappa, B. (2019), *Fracture toughness testing of 6061Al-graphite composites using SENB specimens*, J Inst. Eng. (India), Series D, 100(2): 195-201. doi: 10.1007/s40033-019-00188-z
- Dhummansure, V., Kalyanrao, A.A., Doddamani, S. (2020), *Optimization of process parameters for fracture toughness of Al6061-graphite composites*, Struct. Integ. Life, 20(1): 51-55.

© 2023 The Author. Structural Integrity and Life, Published by DIVK (The Society for Structural Integrity and Life 'Prof. Dr Stojan Sedmak') (<http://divk.inovacionicentar.rs/ivk/home.html>). This is an open access article distributed under the terms and conditions of the [Creative Commons Attribution-NonCommercial-NoDerivatives 4.0 International License](https://creativecommons.org/licenses/by-nc-nd/4.0/)